Systems & Control Transactions

Research Article - Peer Reviewed Conference Proceeding
ESCAPE 35 - European Symposium on Computer Aided Process Engineering
Ghent, Belgium. 6-9 July 2025
Jan F.M. Van Impe, Grégoire Léonard, Satyajeet S. Bhonsale,
Monika E. Polańska, Filip Logist (Eds.)

PSE PRESS

Bayesian Optimization for Enhancing Spherical Crystallization Derived from Emulsions: A Case Study on Ibuprofen

Xinyu Cao[a], Yifan Song[b], Jiayuan Wang[b], Linyu Zhu[b], and Xi Chen[a]*

[a] Zhejiang University, College of Control Science and Engineering, Hangzhou, Zhejiang Province, China
[b] Zhejiang University of Technology, College of Chemical Engineering, Hangzhou, Zhejiang Province, China.
* Corresponding Author: xi_chen@zju.edu.cn.

ABSTRACT

The pharmaceutical industry is a highly specialized field where strict quality control and accelerated time-to-market are essential for maintaining competitive advantage. Spherical crystallization has emerged as a promising approach in pharmaceutical manufacturing, offering significant potential to reduce equipment and operating costs, enhancing drug bioavailability, and facilitating compliance with product quality regulations. Emulsions, as an enabling technology for spherical crystallization, present unique advantages. However, the quality of spherical crystallization products derived from emulsions is significantly influenced by the intricate interactions between crystallization phenomena, formulation variables, and solution hydrodynamics. These complexities pose substantial challenges in determining optimal operational conditions to achieve the desired product characteristics. In this study, Bayesian optimization (BO) is employed to refine and optimize the operational conditions for the spherical crystallization of a representative drug, ibuprofen. The primary goal is to improve product flowability, measured by angle of repose, while maintaining the median particle size within a specified range. The optimization process focuses on key variables such as temperature, stirring speed, duration, and BSA concentration. With the help of acquisition functions, BO enables the identification of a high-quality product with fewer experimental trials compared with traditional design of experiments (DoE) methods.

Keywords: Spherical crystallization, Bayesian optimization.

INTRODUCTION

Spherical crystallization is an innovative technique in pharmaceutical manufacturing that has obtained increasing attention due to its ability to enhance both product quality and process efficiency[1]. By combining crystallization and agglomeration in a single step, spherical crystallization enables the production of spherical crystal forms that are easier to handle and have improved flow properties, which are crucial for downstream processes such as tablet formation and capsule filling[2]. However, the quality of spherical crystallization products obtained from emulsions is highly dependent on the complex interactions between crystallization processes, formulation parameters, and solution hydrodynamics[3]. These interrelated factors introduce significant challenges in determining the optimal operating conditions necessary to achieve the desired product characteristics, such as consistency in particle size and crystal morphology. This complexity underscores the necessity for a carefully structured experimental design[4]. Through such experimentation, it is possible to identify the most favorable conditions, thereby optimizing the process for consistent, high-quality product development.

Traditional experimental design methods, such as one-factor-at-a-time (OFAT) and factorial designs, are widely used to study the effects of process parameters. However, these approaches can be inefficient, particularly when dealing with complex systems where interactions between variables are significant[5]. Definitive screening designs (DSD), in combination with response surface methodology (RSM), offer a more efficient and

comprehensive strategy for process optimization[6]. DSD is particularly effective in identifying the most influential factors with a minimal number of experimental runs, while accounting for potential interactions and nonlinear effects. Once key factors are identified, RSM is applied to further refine the understanding of the process by modeling the relationship between these factors and the desired output. This combined approach allows for an efficient exploration of input spaces.

Building on the efficiency of definitive screening designs and response surface methodology, Bayesian optimization (BO)[7, 8] presents a newer approach for optimizing complex processes in product development. This method offers a more efficient way to explore parameter spaces by using a probabilistic model to guide the selection of the most promising experimental conditions, thus reducing the need for exhaustive testing. This technique has demonstrated considerable potential across multiple domains, including pharmaceutical manufacturing[9], environmental monitoring[10], and the food industry[11]. In the context of spherical crystallization, where multiple interacting variables influence product quality, BO can help identify optimal conditions more quickly, contributing to faster development of new formulations.

This paper presents a comprehensive investigation into the optimization of spherical crystallization processes for pharmaceutical manufacturing. The second section outlines the experimental procedure for the spherical crystallization of a representative drug, ibuprofen, illustrating the practical application of the technique. In the third section, two experimental design methods are discussed: (1) Definitive screening designs combined with response surface methodology, and (2) Bayesian optimization. The fourth section presents and analyzes the experimental results obtained from these approaches. Finally, Potential directions for future research are discussed in the conclusion.

EXPERIMENTAL PROCEDURE: SPHERICAL CRYSTALLIZATION OF IBUPROFEN

This study aims to develop a standard-compliant spherical crystallization product of ibuprofen by optimizing experimental conditions. The spherical crystallization process will be introduced in this section.

Spherical Crystallization Process

The ibuprofen used for spherical crystallization was sourced from *Rhawn* (China). Distilled water and dichloromethane (DCM) (*SCR*, China) were utilized in the crystallization process. Bovine serum albumin (BSA) (*Shyuanye*, China) and quinoa starch served as Pickering particles to stabilize the emulsions. Ethyl cellulose (EC) (*Macklin*, China) was employed as a crystallization additive. The spherical crystallization process was performed in Pickering emulsions, with the procedure adapted from the authors' previously published work[12, 13].

As shown in Fig. 1, an oil-in-water (O/W) emulsion was prepared with dichloromethane as the dispersed phase (which is also the oil phase) and a 0.1 wt% BSA solution as the continuous phase (which is also the aqueous phase). Ibuprofen and EC were dissolved in the oil phase, while quinoa starch was added to the aqueous phase and dispersed via ultrasonication for 10 minutes. The oil and aqueous phases were then combined in a 100 mL round-bottom flask and mixed by handshaking for 1 minute to form the O/W emulsion, after which the Pickering emulsion was obtained. Subsequently, the emulsion was transferred to a 250 mL flask for the evaporation and crystallization processes. Evaporation was carried out in an oil bath (DF-101S, Shanghai Lichenbangxi Instrument Co., Ltd.) equipped with a top stirrer (*WIGGENS*, WB2000-B). Upon completion of crystallization, the resulting product was transferred to a filtration flask and filtered using a recirculating water vacuum pump (SHZ-D (III), Shanghai Lichenbangxi Instrument Co., Ltd.) to remove residual aqueous phase. The product was then washed twice with 100 mL of distilled water and dried in an oven at 50°C for 24 hours. Further analysis of the product includes flowability analysis and particle size analysis.

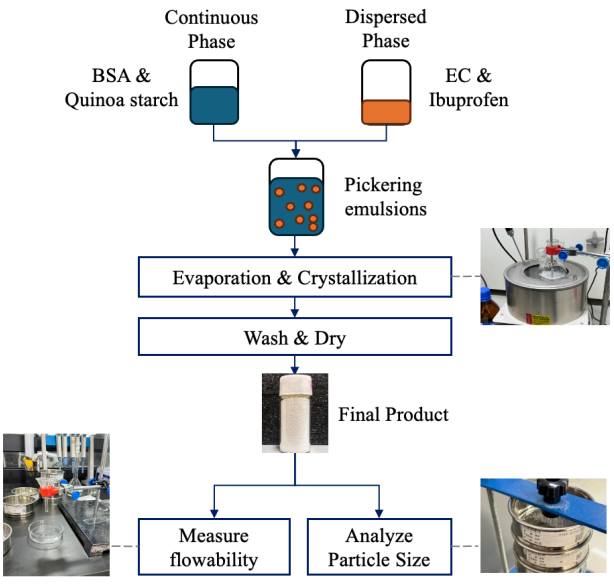

Figure 1. Crystalization process and analysis flowchart .

Flowability Measurements

The flow properties of the spherical agglomerates were assessed indirectly by measuring the angle of repose (AVA). The experimental setup for measuring the angle of repose is illustrated in Fig. 2.

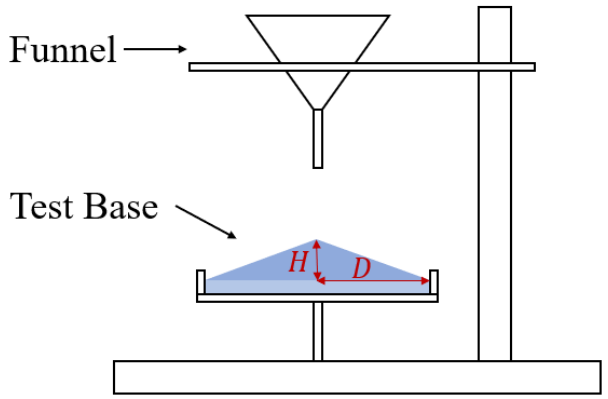

Figure 2. Measurement of the angle of repose.

To minimize the influence of varying compaction states of the powder on measurement accuracy, the powder samples were pre-sieved through a screen with a mesh size of 1.0 mm prior to testing. The funnel used for the measurement had a neck length of 4 cm and a neck diameter of 8 mm. The test base had a diameter of 10 cm and featured a raised edge. To reduce errors caused by particle dispersion upon initial impact, a layer of powder was retained on the base during the test. The angle of repose, denoted as α, was calculated using the formula[2]:

$$\alpha = arctan\left(\frac{H}{D}\right) \quad (1)$$

where H represents the height of the powder cone, and D is the radius of the test base. A lower angle of repose indicates superior flowability. Each sample was measured twice, and the average value was reported to ensure reliability.

Particle Size Analysis

The particle size parameters, marked as d_{10}, d_{50}, and d_{90} of the product were determined through sieving. These parameters represent the 10%, 50%, and 90% points in the cumulative undersize particle size distribution. The analysis was performed using a series of sieves with uniformly spaced apertures ranging from 0.05 to 1 mm, arranged on a standard testing sieve shaker. The sample was introduced onto the top sieve, and the sieving process was carried out using mechanical vibration. Upon completion of the sieving, the particles retained on each sieve layer were carefully weighed and recorded. This data enabled the characterization of the particle size distribution and the calculation of the d_{10}, d_{50}, and d_{90} values.

METHODOLOGY

Product Requirements and Constraints

In the case of spherical crystallization of ibuprofen, AVA is directly linked to its flowability, which is critical for its processing and formulation in pharmaceutical applications. A lower angle of repose indicates better flowability, which is essential for ensuring uniform mixing, accurate dosing, and efficient tableting during production. Good flowability of ibuprofen crystals reduces issues such as clogging in machinery and inconsistent tablet weights. Additionally, controlling the particle size of ibuprofen is vital because it affects not only its flowability but also its dissolution rate and bioavailability. Hence, in our research, the aim is to achieve an angle of repose that is as small as possible while ensuring that the median particle size (d_{50}) falls within a certain range, which is specified of 300-450 μm in this study. The mathematical expression for the optimization problem can be formulated as follows:

$$\min_{\boldsymbol{u}} \ tan(\alpha(\boldsymbol{u})) \quad (2)$$

$$s.t. \ 300 < d_{50}(\boldsymbol{u}) < 450$$

$$\boldsymbol{u}_{lower} < \boldsymbol{u} < \boldsymbol{u}_{upper}$$

where $\boldsymbol{u}$ is the 9-dimensional operating condition shown in Table 1, and $\boldsymbol{u}_{lower}$ and $\boldsymbol{u}_{upper}$ correspond to the lower and upper bound of $\boldsymbol{u}$, respectively. It should be noted that the relationship between the input operating conditions $\boldsymbol{u}$ and output (tan (α) and d_{50}) is unknown, so both the objective function and the constraints are inferred from experimental observations. In addition, the optimization would be performed based on trial data or feedback from experimental results, without a predefined mechanistic model.

Table 1: Experimental conditions $\boldsymbol{u}$ and its upper & lower limits.

No.	Experimental condition	Lower bound	Upper bound
1	Temperature (℃)	40	60
2	Stirring speed (rpm)	300	800
3	Stirring time (min)	10	20
4	Oil-to-water ratio (ml)	0.25	1
5	Starch concentration (g/ml)	3.75	20
6	Bridging agent concentration (mg/ml)	2	15
7	BSA concentration (mg/ml)	0.05	3
8	Ibuprofen concentration (mg/ml)	100	350
9	Total volume (ml)	40	100

Design of Experiments: DSD-RSM Combination

This section outlines how the problem is addressed through the integration of Definitive Screening Designs and Response Surface Methodology. Initially, DSD is employed to conduct 25 experimental runs, which systematically screen the nine factors involved. This screening process facilitates the identification of the two most

influential factors by evaluating their main effects. Through this approach, the number of factors is effectively reduced, focusing on those that significantly impact the response.

In the second phase, RSM is applied to the two factors selected during DSD. To explore the interactions between these two factors and their effects on the response, a set of 20 experimental runs is designed. This number of experiments allows for a thorough investigation of the factor space, ensuring that both linear and quadratic effects, as well as potential interactions, are captured. Specifically, the process begins with 10 experimental runs to refine the upper and lower bounds of the two factors identified in the screening phase. Subsequently, 10 additional experiments are conducted using Central Composite Design (CCD), a specific approach within RSM, to explore the relationship between the factors within the newly established boundaries. This CCD phase consists of 9 factorial points and 1 center point. The factorial points represent all possible combinations of the three levels (low, center, and high) for each of the two selected factors with newly established boundaries. These points allow for a detailed exploration of the main effects, as well as the quadratic and interaction effects between the factors.

Bayesian Optimization

In both DSD and RSM methods, experiments are designed at once based on the input space. At the same time, no handling of constraints is performed. This section primarily discusses how BO can adaptively replace the traditional experimental design methods mentioned above, while also addressing unknown constraints.

BO works by constructing a surrogate model (which is a Gaussian Process model in this work) to predict the target function, and it uses a balance between exploration and exploitation to select the next points most likely to improve the objective function, thus efficiently finding the optimal solution. The acquisition function plays a crucial role in determining the next sampling point. It helps balance "exploration" (searching unknown areas of the design space) and "exploitation" (focusing on areas known to give high objective function values). The Lower Confidence Bound (LCB) is one of the acquisition functions used in Bayesian optimization, particularly with Gaussian Process (GP) regression models. LCB is based on a trade-off between the predicted mean and the uncertainty of the target function, allowing for exploration of uncertain regions while also exploiting known good areas. In our problem, the LCB acquisition function can be expressed as follows:

$$\min_{\boldsymbol{u}} \ \mu(\boldsymbol{u}) - \rho.\sigma(\boldsymbol{u}) \tag{3}$$

where μ and σ are the mean and variance of $\tan(\alpha)$ inferred from GP, and ρ is a hyperparameter that controls the balance between exploration and exploitation. While a higher value of ρ encourages exploration of areas with high uncertainty, a lower value encourages exploiting regions with known good performance. Exploration may be more important because GP will have more uncertainty in its predictions initially. Over time, as the model becomes more confident about the objective function's shape, more exploitation can be encouraged. Thus, ρ is related to experimental step N in this paper. Their relationship is as follows:

$$\rho = e^{-\frac{N}{10}+1} \tag{4}$$

As for the constraints, GP is also built for d_{50}. In this way, the probability density functions can be calculated, ensuring that the probability of constraints being satisfied is within a given interval[14]. Here, the probability of satisfying the unknown constraints is set to be greater than 80%. Therefore, the acquisition function is updated with the following two additional constraints. They can be expressed as follows:

$$\begin{aligned} &\min_{\boldsymbol{u}} \ \mu(\boldsymbol{u}) - e^{-\frac{N}{10}+1}.\sigma(\boldsymbol{u}) \\ &s.t. \ p(\,d_{50} > 300) > 80\% \\ &\qquad p(\,d_{50} < 450) > 80\% \end{aligned} \tag{5}$$

where $p(.)$ represents he probability density function. Before the optimization process begins, 10 experimental points (e.g., operating condition $\boldsymbol{u}$) will be initially sampled using the Latin Hypercube Sampling method to construct the preliminary GP model. Starting from the 11th point, each subsequent experimental point will be selected sequentially based on Eq. (5).

RESULT & DISCUSSION

This section examines the outcomes of two experimental design methodologies: traditional DoE and BO. The experimental results for the DSD-RSM combination method are presented in Table 2, while those for BO are detailed in Table 3. Physical insights are also presented.

Result of DSD-RSM Combination

As shown in Fig. 3, firstly in DSD, two relatively important factors were identified: stirring speed and oil-to-water ratio through DSD. Subsequently, 10 experimental runs were conducted to refine the bound for stirring speed from [300, 800] to [400, 600], and for oil-to-water ratio from [0.25, 1] to [0.6, 1], as illustrated in Table 2. After narrowing the ranges for these key factors, an additional 10 experiments were performed using CCD, a three-level design focusing on stirring speed values of 400, 500, and 600, and oil-to-water ratio values of 0.6, 0.8, and 1, respectively. The experimental results in Table 2 indicate that the smallest AVA identified using the DSD-

Table 2: Experimental results of traditional DoE.

No.	Temperature	Stirring speed	Stirring time	Oil-to-water ratio	Starch concentration	Bridging agent concentration	BSA concentration	Ibuprofen concentration	Total volume	d_{50}	$\tan(\alpha)$
Definitive Screening Design											
1	40	800	10	0.25	3.75	0.015	3	0.35	40	219.6	40.05
2	60	800	10	1	20	0.002	3	0.1	40	133.8	41.37
3	60	800	10	0.625	20	0.015	0.05	0.35	100	359.7	38.08
4	60	800	30	1	3.75	0.002	0.05	0.35	40	277.4	39.53
5	60	600	30	0.25	20	0.015	3	0.1	40	254.9	39.39
6	40	800	10	1	11.875	0.015	0.05	0.1	40	236.3	39.63
7	60	800	10	0.25	3.75	0.002	3	0.225	100	189.3	40.72
8	60	400	10	1	3.75	0.015	1.525	0.1	100	428.6	36.42
9	60	400	30	1	20	0.002	0.05	0.1	100	504.2	36.42
10	60	800	30	0.25	3.75	0.015	0.05	0.1	70	163.2	41.02
11	50	400	10	0.25	3.75	0.002	0.05	0.1	40	223.1	39.87
12	60	400	20	1	3.75	0.015	3	0.35	40	603.4	37.24
13	40	800	30	0.25	20	0.002	1.525	0.35	40	173.1	40.59
14	40	800	30	1	3.75	0.0085	3	0.1	100	241.3	39.58
15	50	600	20	0.625	11.875	0.0085	1.525	0.225	70	243.5	38.44
16	40	600	10	1	3.75	0.002	0.05	0.35	100	464.3	36.76
17	50	800	30	1	20	0.015	3	0.35	100	427.0	35.88
18	40	400	10	0.25	20	0.015	3	0.1	100	139.6	41.03
19	40	400	10	1	20	0.002	3	0.35	70	493.6	36.37
20	60	400	10	0.25	20	0.0085	0.05	0.35	40	370.5	37.48
21	40	400	30	0.625	3.75	0.002	3	0.1	40	470.3	35.71
22	40	800	20	0.25	20	0.002	0.05	0.1	100	546.6	38.82
23	60	400	30	0.25	11.875	0.002	3	0.35	100	428.6	35.88
24	40	400	30	0.25	3.75	0.015	0.05	0.35	100	537.3	36.75
25	40	400	30	1	20	0.015	0.05	0.225	40	399.5	36.94
Response Surface Methodology											
1	50	400	20	0.6	11.875	0.015	1.525	0.225	70	383.5	37.58
2	50	500	20	0.6	11.875	0.015	1.525	0.225	70	428.7	36.67
3	50	600	20	0.6	11.875	0.015	1.525	0.225	70	267.6	37.60
4	50	700	20	0.6	11.875	0.015	1.525	0.225	70	249.9	38.55
5	50	800	20	0.6	11.875	0.015	1.525	0.225	70	255.3	38.67
6	50	500	20	0.25	11.875	0.015	1.525	0.225	70	293.8	38.87
7	50	500	20	0.42	11.875	0.015	1.525	0.225	70	337.2	37.84
8	50	500	20	0.6	11.875	0.015	1.525	0.225	70	428.7	36.67
9	50	500	20	0.8	11.875	0.015	1.525	0.225	70	442.8	35.78
10	50	500	20	1	11.875	0.015	1.525	0.225	70	508.2	35.19
11	50	600	20	1	11.875	0.015	1.525	0.225	70	421.7	36.47
12	50	500	20	0.8	11.875	0.015	1.525	0.225	70	459.8	35.63
13	50	400	20	0.6	11.875	0.015	1.525	0.225	70	383.5	37.58
14	50	500	20	0.6	11.875	0.015	1.525	0.225	70	428.7	36.67
15	50	600	20	0.8	11.875	0.015	1.525	0.225	70	402.5	36.53
16	50	500	20	1	11.875	0.015	1.525	0.225	70	508.2	35.19
17	50	400	20	0.8	11.875	0.015	1.525	0.225	70	473.9	36.89
18	50	400	20	1	11.875	0.015	1.525	0.225	70	404.7	36.60
19	**50**	**500**	**20**	**0.8**	**11.875**	**0.015**	**1.525**	**0.225**	**70**	**442.8**	**35.78**
20	50	600	20	0.6	11.875	0.015	1.525	0.225	70	267.6	37.60

RSM combination, while meeting the d_{50} constraints, occurs at the center point of the CCD phase with the value of 35.78. Interestingly, this center point was tested twice during the CCD phase—once satisfying the constraints and once failing to do so (see "Response Surface Methodology", No. 12 and 19 in Table 2). This is because each experiment inevitably involved some deviations. The d_{50} boundary we set ranges from 300 to 450 μm. In the two repeated experiments, one yielded a d_{50} value of 442.8, while the other resulted in 459.8. This also indicates that under the experimental conditions of 12th and 19th runs, d_{50} is generally close to the upper boundary of 450.

The experimental results align with the underlying physical principles governing the crystallization process. Higher stirring speed results in finer particles with rougher surfaces, increasing friction and reducing flowability. However, very low stirring speeds can lead to unsuccessful crystallization. Meanwhile, a higher oil-to-water ratio improves size uniformity, enhancing flowability through reduced friction and narrower particle size distribution. To conclude, these two factors—stirring speed and oil-to-water ratio—significantly affect both d_{50} and

Table 3: Experimental results of BO.

No.	Temperature	Stirring speed	Stirring time	Oil-to-water ratio	Starch concentration	Bridging agent concentration	BSA concentration	Ibuprofen concentration	Total volume	d_{50}	$\tan(\alpha)$
1	52.62	592.82	13.47	0.64	6.13	15.00	2.38	113.41	73.28	330.60	38.47
2	42.47	416.80	15.31	0.56	7.29	2.87	2.44	150.01	83.92	285.00	38.86
3	**58.31**	**452.50**	**12.09**	**0.74**	**16.52**	**7.05**	**2.73**	**312.25**	**93.78**	**397.60**	**35.84**
4	46.97	645.45	17.96	0.80	9.98	9.92	2.73	246.26	44.51	394.10	36.34
5	55.92	656.39	11.61	0.47	18.31	11.66	0.48	214.30	47.52	304.80	38.07
6	49.87	741.03	14.95	0.54	18.55	9.36	1.93	250.12	77.02	303.50	38.39
7	50.61	769.89	18.13	0.36	14.22	5.27	0.90	341.40	63.19	301.30	38.75
8	57.59	546.06	16.75	0.94	4.90	7.32	1.18	132.18	65.79	533.80	35.12
9	44.32	380.83	10.57	0.85	12.22	12.92	1.26	280.98	95.67	564.80	37.27
10	40.53	344.16	19.94	0.26	11.41	3.96	1.64	186.97	56.35	232.70	39.62
11	60.00	602.57	20.00	1.00	3.75	5.33	0.13	145.05	57.42	418.40	35.97
12	41.54	760.26	20.00	1.00	6.65	2.49	3.00	279.11	89.00	284.40	38.89
13	46.87	629.18	20.00	1.00	5.26	8.06	3.00	252.84	40.00	398.15	36.59
14	40.00	669.12	20.00	0.54	20.00	14.48	3.00	256.25	63.55	157.00	40.82
15	60.00	610.82	20.00	1.00	3.75	2.00	3.00	141.33	40.00	242.58	39.20
16	56.69	590.76	19.36	1.00	3.75	12.27	0.05	114.77	91.92	421.39	36.35
17	50.71	675.59	12.08	0.84	3.75	10.05	0.05	231.44	43.52	210.05	39.89
18	60.00	600.24	20.00	1.00	3.75	5.60	0.05	145.42	59.70	395.15	36.30
19	60.00	471.27	12.47	0.71	17.70	5.50	3.00	320.76	93.37	381.73	36.15
20	57.12	443.52	11.91	0.75	15.96	7.79	2.58	308.24	93.99	395.97	36.45
21	58.93	460.41	12.25	0.73	17.02	6.39	2.81	315.85	93.61	402.42	36.05
22	60.00	604.58	20.00	1.00	3.75	5.22	0.05	146.70	56.40	342.46	37.25
23	60.00	456.00	12.54	0.97	15.74	7.17	3.00	308.60	92.15	451.44	35.88
24	58.65	453.82	12.13	0.74	16.57	6.95	2.78	312.69	93.70	390.2	36.00
25	56.73	449.72	12.03	0.74	16.37	7.27	2.54	311.13	93.88	396.7	36.21

α, and they were selected as critical variables in the experimental design. For stirring speed, a lower value tends to produce larger particles with smoother surface comparing to the fines, which corresponds to the smaller values observed in our optimized results. The initial range was 300 to 800, with 500 as the traditional experimental design value. For the oil-to-water ratio, a relatively higher value produces more uniform particles. The initial range was 0.25 to 1, and the traditional experimental design value was 0.8.

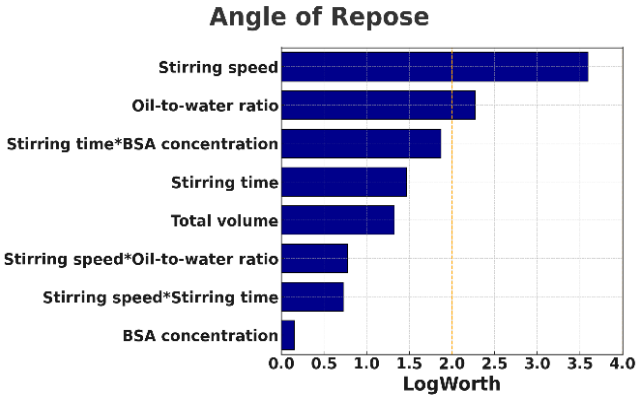

Figure 3. Analysis of definitive screening design.

Result of BO

As illustrated in Table 3, the smallest AVA identified while meeting the d_{50} constraints using BO occurs at the third experiments, with the value of 35.84. In the sequential Bayesian experiments, runs 19, 20, 21, 23, 24, and 25 were all very close to the third experimental design. This indicates that the Bayesian optimization is nearing convergence. However, it is unfortunate that despite searching around the current optimal region, no experimental condition was found that outperforms the result of 35.84 achieved in the third run.

Comparing BO to DSD-RSM combination where a total of 45 experiments were conducted, BO only required 25 experiments, thus saving 55% of the experimental time up to 80 hours. In BO, 16 out of 25 experiments satisfied the constraints, resulting in a proportion of 64%. In contrast, in the DoE, 18 out of 45 experiments satisfied the constraints, with a proportion of 40%. In terms of costs, optimizing spherical crystallization conserves nearly half of the solvent and drug materials, making it highly efficient in resource usage.

At the same time, BO shows consistency with DSD-RSM combination in the final optimization results. The ranges for the two key variables identified through DSD-RSM combination: stirring speed [400, 600] and oil-to-water ratio [0.6, 1]. The optimal experimental values obtained through BO for stirring speed and oil-to-water ratio are 452.5 and 0.74, respectively. In the last 8 experiments of BO, 7 of the experiments yielded data within this range.

CONCLUSION

In summary, this study compared two experimental design methods: the traditional DoE and BO, to identify the optimal conditions for stirring speed and oil-to-water ratio. Overall, both methods produced similar optimal values, with BO providing a more efficient way to identify optimal conditions while maintaining reliability. It is important to note that the research in this paper is purely data-driven, and the integration of mechanistic insights could provide additional improvements in the optimization process. Therefore, future research may focus on incorporating mechanistic knowledge into BO to enhance the efficiency of experimental design. For example, if key factors influencing experimental outcomes are known in advance through mechanistic knowledge, the focus can be directed toward these critical factors, thereby reducing the number of experiments required. Additionally, the presence of a mechanistic model may accelerate the experimental process further.

ACKNOWLEDGEMENTS

Financial support of the "Pioneer" and "Leading Goose" R&D Program of Zhejiang (No. 2024C01028) and the State Key Laboratory of Industrial Control Technology, China (No. ICT2024C04) are gratefully acknowledged.

REFERENCES

1. Saini, S., *Spherical Crystallization: An Overview.* Int. J. Drug Delivery Technol, 2014. **4**(4): p. 72-80 https://www.researchgate.net/publication/267155019_Spherical_Crystallization_An_Overview.
2. Bharti, N., et al., *Spherical crystallization: a novel drug delivery approach.* Asian journal of biomedical and pharmaceutical sciences, 2013. **3**(18): p. 10
3. Kovačič, B., F. Vrečer, and O. Planinšek, *Spherical crystallization of drugs.* Acta pharmaceutica, 2012. **62**(1): p. 1-14 https://sciendo.com/article/10.2478/v10007-012-0010-5.
4. Gyulai, O., et al., *Optimization of the Critical Parameters of the Spherical Agglomeration Crystallization Method by the Application of the Quality by Design Approach.* Materials, 2018. **11**(4) https://www.mdpi.com/1996-1944/11/4/635.
5. Czitrom, V., *One-Factor-at-a-Time versus Designed Experiments.* The American Statistician, 1999. **53**(2): p. 126-131 https://www.tandfonline.com/doi/abs/10.1080/00031305.1999.10474445.
6. Köçkar, H. and N. Kaplan, *Investigation of soft magnetic properties of Ni/Cu multilayer films: Definitive screening design and response surface methodology.* Journal of Materials Science: Materials in Electronics, 2021. **32**(16): p. 20955-20964 https://doi.org/10.1007/s10854-021-06506-0.
7. Shahriari, B., et al., *Taking the Human Out of the Loop: A Review of Bayesian Optimization.* Proceedings of the IEEE, 2016. **104**(1): p. 148-175 https://doi.org/10.1109/JPROC.2015.2494218.
8. Frazier, P.I.J.a.e.-p., *A Tutorial on Bayesian Optimization.* 2018: p. arXiv:1807.02811 https://ui.adsabs.harvard.edu/abs/2018arXiv180702811F.
9. Sano, S., et al., *Application of Bayesian optimization for pharmaceutical product development.* Journal of Pharmaceutical Innovation, 2020. **15**: p. 333-343 https://link.springer.com/article/10.1007/s12247-019-09382-8.
10. Marchant, R. and F. Ramos, *Bayesian optimisation for intelligent environmental monitoring.* p. 2242-2249 https://ieeexplore.ieee.org/document/6385653.
11. Junge, K., et al., *Improving Robotic Cooking Using Batch Bayesian Optimization.* IEEE Robotics and Automation Letters, 2020. **5**(2): p. 760-765 https://ieeexplore.ieee.org/document/8954776.
12. Wang, J., et al., *A Novel Spherical Crystallization Method Using Pickering Emulsions.* Journal of Pharmaceutical Sciences, 2022. **111**(6): p. 1625-1632 https://www.sciencedirect.com/science/article/pii/S0022354921005694.
13. Song, Y., et al., *Quinoa starch-based Pickering emulsions with small-molecule oil solvents: Exploring solvent varieties and depletion attraction.* Chemical Engineering Science, 2024. **299**: p. 120545 https://www.sciencedirect.com/science/article/pii/S0009250924008455.
14. Gelbart, M.A., J. Snoek, and R.P. Adams, *Bayesian Optimization with Unknown Constraints.* 2014 https://doi.org/10.48550/arXiv.1403.5607.